

Supporting Information for

Short Communication

Antitumor synergism between PAK4 silencing and immunogenic phototherapy of engineered extracellular vesicles

Mei Lu^{a,b,†}, Haonan Xing^{b,c,†}, Wanxuan Shao^a, Pengfei Wu^a, Yuchuan Fan^a, Huining He^d, Stefan Barth^e, Aiping Zheng^c, Xing-Jie Liang^{b,*}, Yuanyu Huang^{a,*}

^a*Advanced Research Institute of Multidisciplinary Science, School of Life Science, School of Medical Technology, Key Laboratory of Molecular Medicine and Biotherapy, Key Laboratory of Medical Molecule Science and Pharmaceutics Engineering, Beijing Institute of Technology, Beijing 100081, China*

^b*Chinese Academy of Sciences (CAS) Key Laboratory for Biomedical Effects of Nanomaterials and Nanosafety, CAS Center for Excellence in Nanoscience, National Center for Nanoscience and Technology of China, Beijing 100190, China*

^c*State Key Laboratory of Toxicology and Medical Countermeasures, Beijing Institute of Pharmacology and Toxicology, Beijing 100850, China*

^d*Tianjin Key Laboratory on Technologies Enabling Development of Clinical Therapeutics and Diagnostics, School of Pharmacy, Tianjin Medical University, Tianjin 300070, China*

^e*South African Research Chair in Cancer Biotechnology, Institute of Infectious Disease and Molecular Medicine (IDM), Department of Integrative Biomedical Sciences, Faculty of Health Sciences, University of Cape Town, Anzio Road, Observatory, Cape Town 7925, South Africa*

Received 1 January 2023; received in revised form 4 March 2023; accepted 16 March 2022

[†]These authors made equal contribution to this work.

*Corresponding authors. Tel.: +86 (0)10 68911089 (Yuanyu Huang); +86 (0)10 82545569 (Xing-Jie Liang).

E-mail addresses: yyhuang@bit.edu.cn (Yuanyu Huang), liangxj@nanoctr.cn

(Xing-Jie Liang).

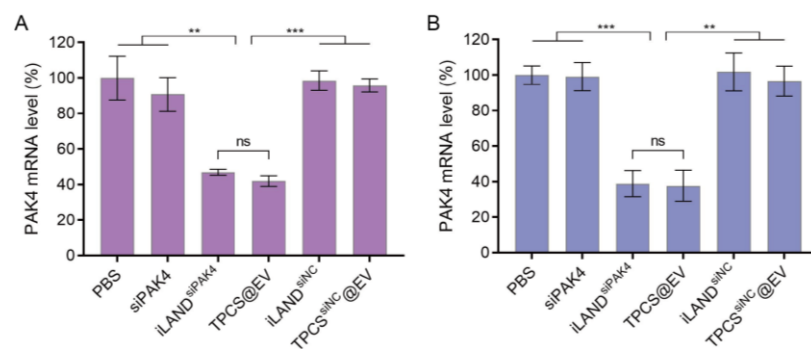


Figure S1 The PAK4 knockdown efficiency of the individual PAK4 silencing (iLAND^{siPAK4}) and the combined treatment (TPCS@EV) in B16F10 cells (A) and the tumor tissues of B16F10 tumor-bearing C57BL/6J mice (B) at the siPAK4 concentration of 100 nM, as determined by qRT-PCR. Data are represented as mean \pm SD ($n = 3$). ** $P < 0.01$, *** $P < 0.001$. ns, not significant.

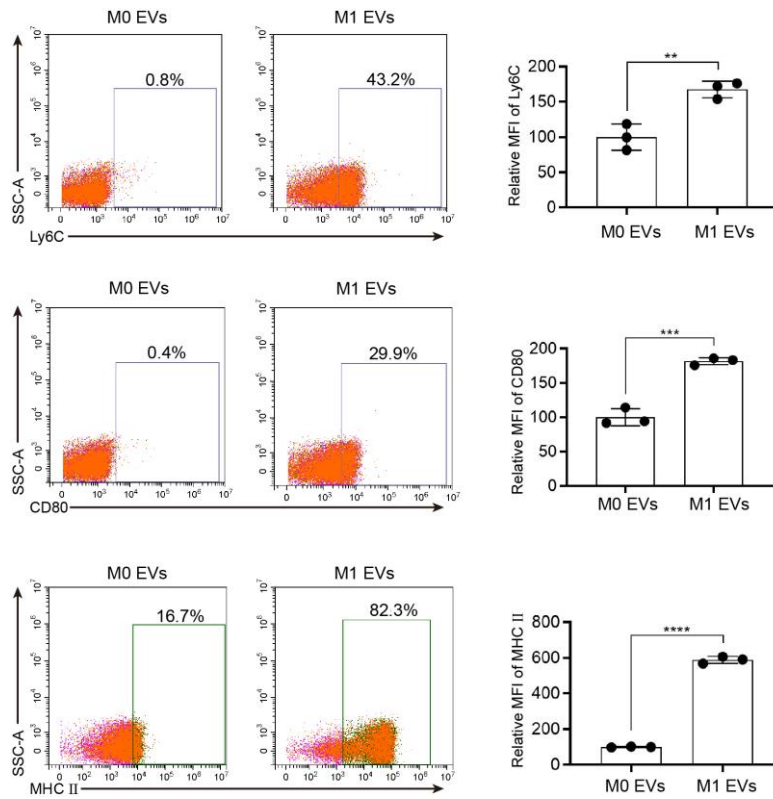


Figure S2 Characterization of the relative expression of the proinflammatory markers (*i.e.*, CD80, MHCII, and Ly6C) of M0 (M0 EVs) and M1 (M1 EVs) macrophage-derived EVs. MFI, mean fluorescence intensity. Data are represented as mean \pm SD ($n = 3$). ** $P < 0.01$, *** $P < 0.001$, **** $P < 0.0001$.

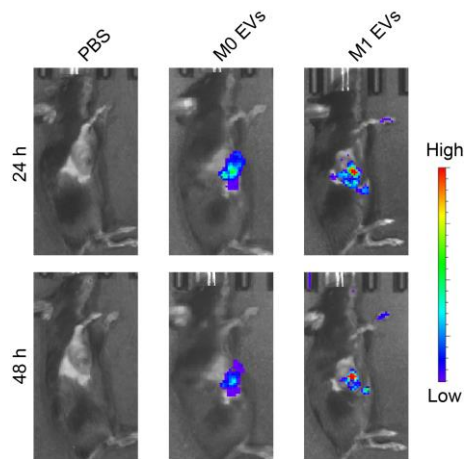


Figure S3 Evaluation of the tumor tropism of M0 (M0 EVs) and M1 (M1 EVs) macrophage-derived EVs in B16F10 tumor-bearing C57BL/6J mice by *in vivo* fluorescence imaging. Phosphate buffer saline (PBS) was taken as the control.

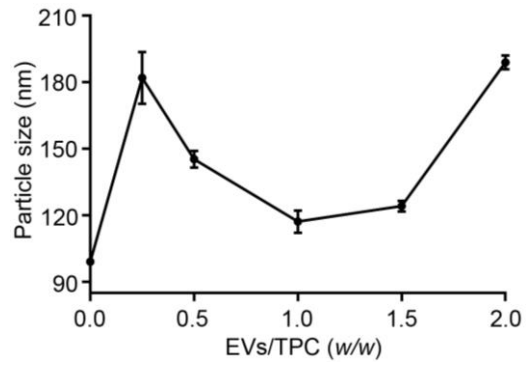


Figure S4 The particle size of the engineered extracellular vesicles (TPCS@EV) at different weight ratios between EVs and the photoactivatable polyethyleneimine (TPC). Data are represented as mean \pm SD ($n=3$).

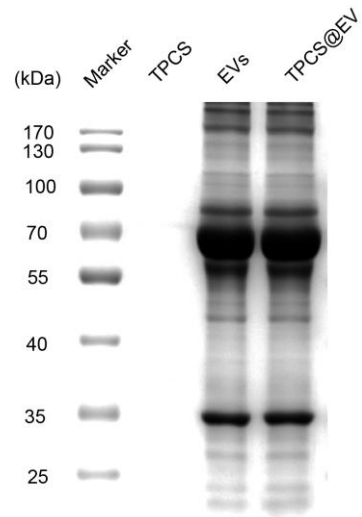


Figure S5 Sodium dodecyl sulfate-polyacrylamide gel electrophoresis (SDS-PAGE) analysis of the protein patterns of TPCS nano-complexes, EVs, and the engineered EVs (TPCS@EV).

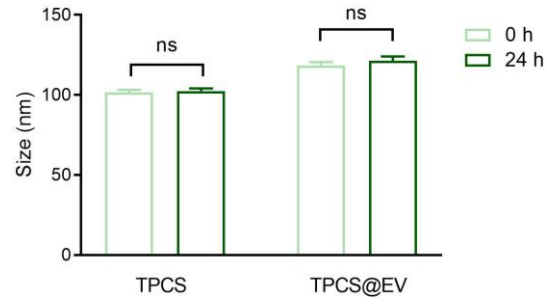


Figure S6 The stability of TPCS@EV in phosphate buffer saline (PBS) after storing at room temperature away from light for 24 h. Data are represented as mean \pm SD ($n = 3$). ns, not significant.

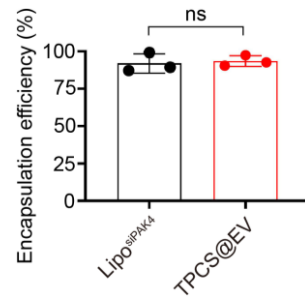


Figure S7 The encapsulation efficiency of siPAK4 by TPCS@EV and Lipo 2000, as determined by the Quant-iT RiboGreen RNA assay. Data are represented as mean \pm SD ($n = 3$). ns, not significant.

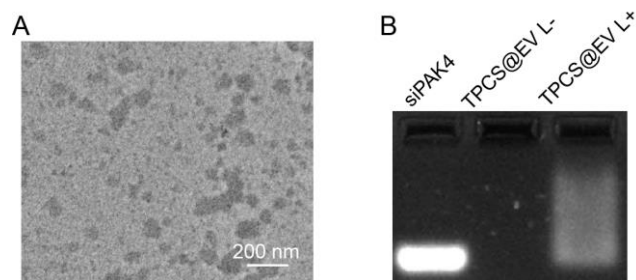


Figure S8 The reactive oxygen species (ROS)-responsive property of TPCS@EV. (A) The TEM image of TPCS@EV following laser irradiation. (B) Analysis of the ROS-responsive siRNA release by using the agarose gel retardation assay.

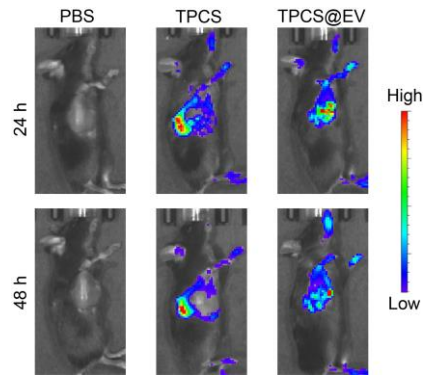


Figure S9 The tumor accumulation of TPCS and TPCS@EV in B16F10 tumor-bearing C57BL/6J mice after intravenous administration. Phosphate buffer saline (PBS) was taken as the control.

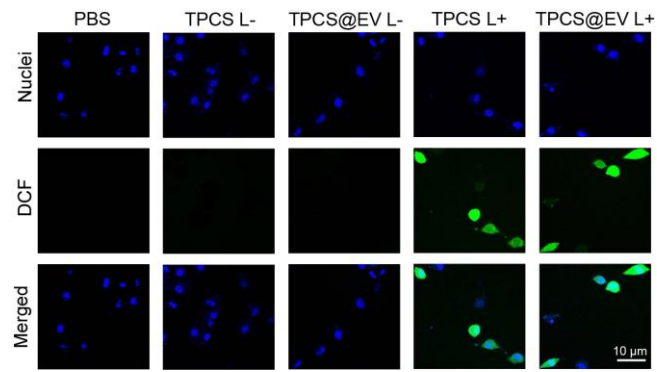


Figure S10 Fluorescence imaging of reactive oxygen species (ROS) generated in B16F10 cells after being treated with TPCS nano-complexes and the engineered EVs (TPCS@EV) in the absence or presence of laser irradiation. Blue, cell nuclei. Green, 2,7-dichloro-fluorescein (DCF), which reflects the level of intracellular ROS.

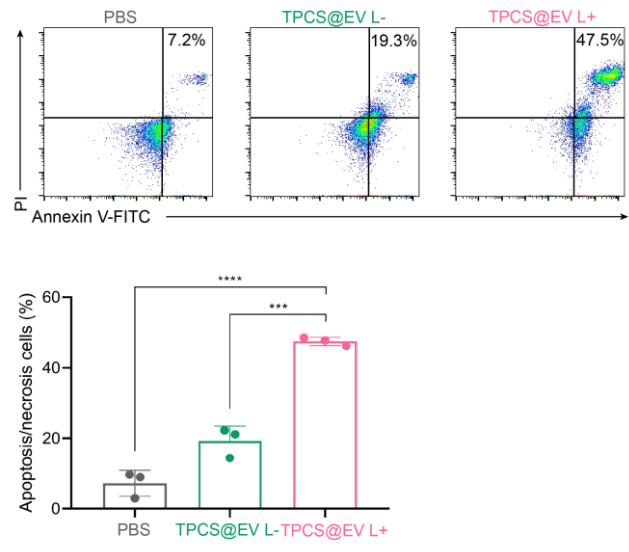


Figure S11 The antitumor activity of the engineered EVs (TPCS@EV) in B16F10 cells, as determined by Annexin V-FITC/PI staining. Data are represented as mean \pm SD ($n = 3$). *** $P < 0.001$, **** $P < 0.0001$.

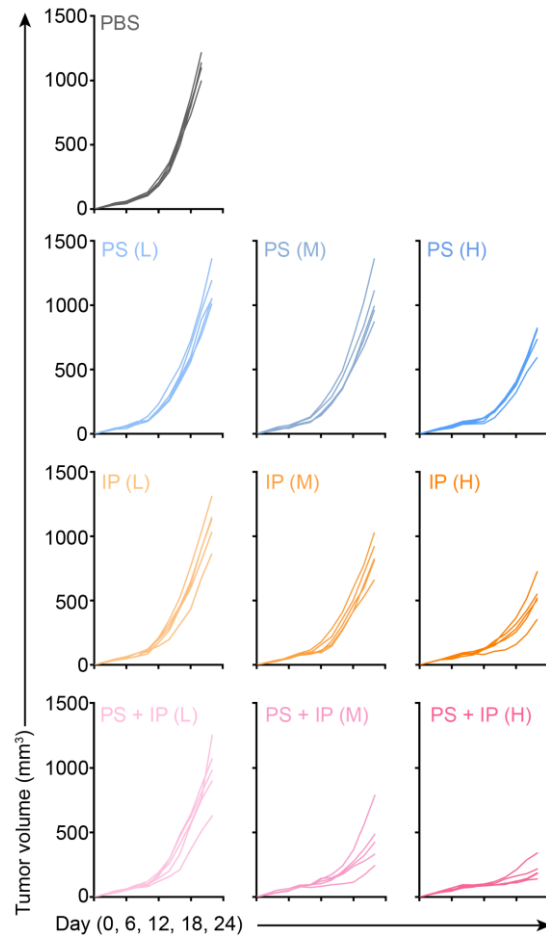


Figure S12 The individual tumor growth curves of B16F10 tumor-bearing mice after being treated with PAK4 silencing alone (PS), immunogenic phototherapy alone (IP) and the combined PAK4 silencing and immunogenic phototherapy (PS + IP) at different siRNA doses (L, 0.25 mg/kg; M, 0.5 mg/kg; H, 1 mg/kg) ($n = 5$).

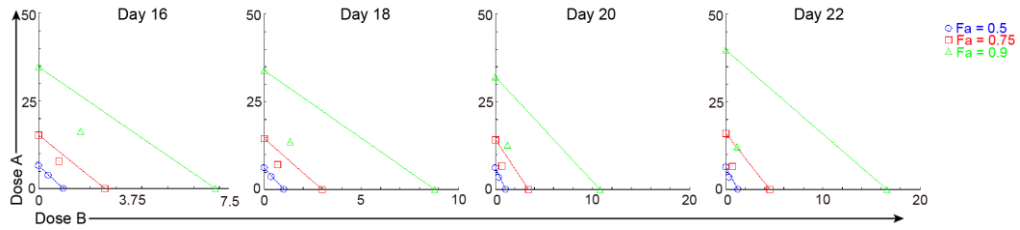


Figure S13 Isobolograms for the combined PAK4 silencing and immunogenic phototherapy of the engineered EVs (TPCS@EV) at 50%, 75%, and 90% inhibition of tumor volume in B16F10 tumor-bearing C57BL/6J mice on Days 16, 18, 20, and 22, as determined by the CompuSyn software. The combination data points on the diagonal (hypotenuse) line, the lower left and upper right suggest additive effects, synergism, and antagonism, respectively. Fa, Fraction affected.

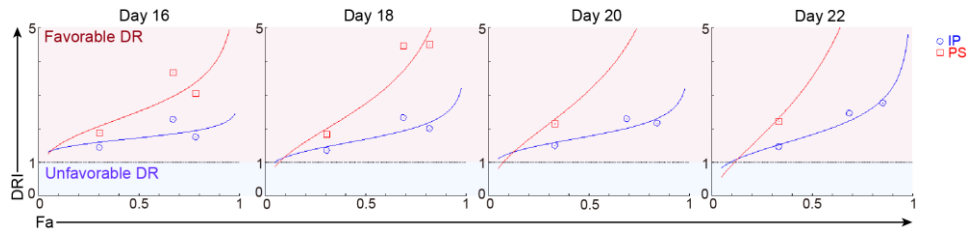


Figure S14 The Fa-DRI plot for the combined treatment of PAK4 silencing (PS) and immunogenic phototherapy (IP) against B16F10 xenograft tumor in C57BL/6J mice on Days 16, 18, 20, and 22, as determined by the CompuSyn software. The dose reduction index (DRI) values $>$, $=$, and $<$ 1 suggest favorable dose reduction (DR), no dose reduction, and unfavorable dose reduction, respectively. Fa, Fraction affected.

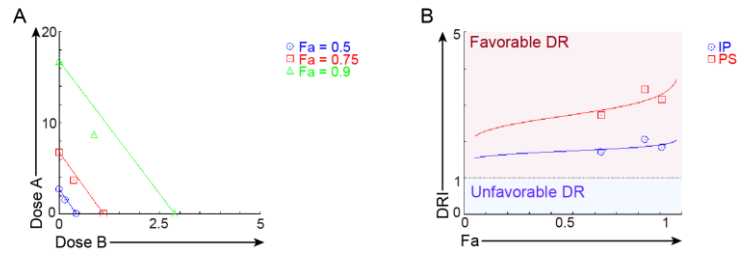


Figure S15 (A) The isobologram for the combined PAK4 silencing (PS) and immunogenic phototherapy (IP) of the engineered EVs (TPCS@EV) at 50%, 75%, and 90% inhibition of tumor weight in B16F10 tumor-bearing C57BL/6J mice. (B) The Fa-DRI plot for the combined treatment for inhibition of tumor weight in B16F10 tumor-bearing C57BL/6J mice. Fa, Fraction affected.

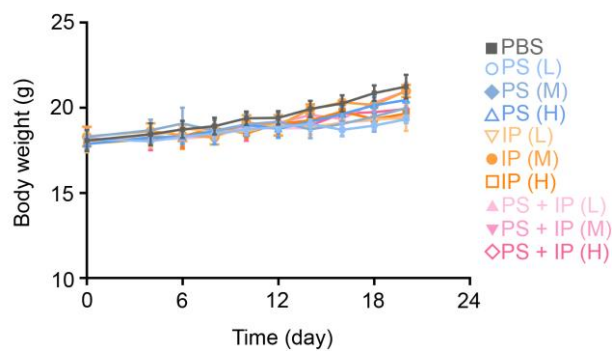


Figure S16 Body weight variation of B16F10 tumor-bearing C57BL/6J mice during the treatment course of individual PAK4 silencing (PS), individual immunogenic phototherapy (IP), and the combined PAK4 silencing and immunogenic phototherapy (PS + IP) at different siRNA doses (L, 0.25 mg/kg; M, 0.5 mg/kg; H, 1 mg/kg). Data are represented as mean \pm SD ($n = 3$).

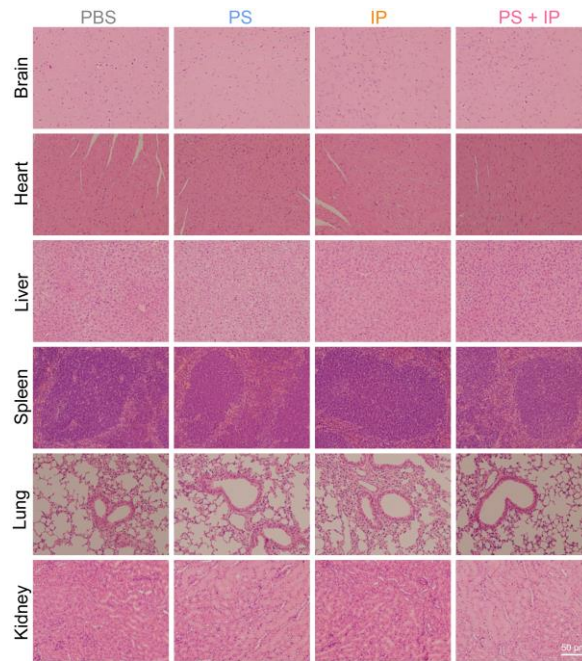


Figure S17 Hematoxylin and Eosin (H&E) staining of the major organs harvested from B16F10 tumor-bearing mice following different treatments at the siRNA doses of 1 mg/kg. PS, individual PAK4 silencing. IP, individual immunogenic phototherapy. PS + IP, the combined treatment of PAK4 silencing and immunogenic phototherapy.

Notes: ED₅₀, median effective dose; ED₇₅, 75% effective dose; ED₉₀, 90% effective dose; ED₉₅, 95% effective dose.

CI, combination index. CI values <, =, and >1 suggest synergism, additive effect, and antagonism, respectively.

DRI, dose reduction index. The DRI value indicates the folds of dose reduction that allowed in the combined therapy for a given degree of effect, as compared to the dose of each therapy alone.

PS, individual PAK4 silencing.

IP, individual immunogenic phototherapy.

PS + IP, the combined treatment of PAK4 silencing and immunogenic phototherapy.